文章编号: 0254 - 5357(2009)01 - 0053 - 16

Laser Ablation-Inductively Coupled Plasma-Mass Spectrometry and Its Application in Geochemistry, Cosmochemistry and Environmental Research

JOCHUM Klaus Peter[1], *STOLL Brigitte*[1], *FRIEDRICH Jon M*[2,3], *AMINI Marghaleray*[1,4], *BECKER Stefan*[5], *DüCKING Marc*[5], *EBEL Denton S*[2], *ENZWEILER Jacinta*[6], *HU Ming-yue*[7], *KUZMIN Dmitry*[1,10], *MERTZ-KRAUS Regina*[1,8], *MüLLER Werner E G*[9], *REGNERY Julia*[1], *SOBOLEV Alexander*[11,1], *WANG Xiao-hong*[1,7], *ZHAN Xiu-chun*[7]

(1. Max Planck-Institut für Chemie, Mainz 55020, Germany;
2. Department of Earth and Planetary Sciences, American Museum of Natural History, New York 10024, USA;
3. Department of Chemistry, Fordham University, Bronx, New York 10458, USA;
4. Saskatchewan Isotope Laboratory, Department of Geological Sciences, University of Saskatchewan, Saskatoon S7N 5E2, Canada;
5. Bundeskriminalamt, Wiesbaden 65173, Germany;
6. Instituto de Geociências, University of Campinas, CP 6152 Campinas, CEP 13083-970, Brazil;
7. National Research Center for Geoanalysis, Beijing 100037, China;
8. Institut für Geowissenschaften, Universität Mainz, Mainz 55099, Germany;
9. Institut für Physiologische Chemie, Universität Mainz, Mainz 55099, Germany;
10. Institute of Geology and Mineralogy, Siberian Branch of Russian Academy of Sciences, Novosibirsk 630090, Russia;
11. V. I. Vernadsky Institute of Geochemistry and Analytical Chemistry, Russian Academy of Sciences, Moscow 119991, Russia)

Abstract: Laser ablation (LA)-inductively coupled plasma-mass spectrometry (ICP-MS) has become one of the most important methods for *in situ* trace elemental and isotopic analysis in geochemistry, cosmochemistry and environmental research. For these purposes, different kinds of mass spectrometers and lasers are used, which are presented in this paper. One of the most useful LA-ICPMS instruments is the combination of a single-collector sector field mass spectrometer with Nd: YAG laser ablation systems (193 nm and 213 nm wavelengths, respectively). This design used in the MPI Mainz laboratory is described in detail in this paper. Data optimization techniques including diverse correction procedures are also discussed. To demonstrate the power of LA-ICPMS, several applications of trace elemental and isotopic analysis are presented, such as investigations of reference materials, trace element analysis in Hawaiian basalts, Martian meteorites, biological spicules and corals, as well as Pb and Sr isotope measurements of melt inclusions and Ca-Al rich inclusions of carbonaceous chondrites.

Key words: laser ablation-inductively coupled plasma-mass spectrometry (LA-ICPMS); geological sample; reference material; meteorite; biological sample; trace element; isotope ratio

收稿日期: 2008-05-26; 修订日期: 2008-08-07

作者简介: JOCHUM Klaus Peter, major in trace element and isotope geochemistry (mainly oceanic basalts, meteorites, environmental and biological samples), LA-ICPMS, investigations of reference materials, GeoReM database. E-mail: kpj@mpch-mainz.mpg.de。

激光剥蚀 - 等离子体质谱技术及其在地球化学宇宙化学和环境研究中的应用

摘要：激光剥蚀 - 等离子体质谱(LA - ICPMS)已成为地球化学、宇宙化学和环境研究领域元素和同位素原位分析最重要的技术之一。文章介绍了多种类型的质谱仪及其使用的激光器。用途最广的LA - ICPMS仪器之一是单接收器扇形磁场质谱仪,配有 Nd:YAG 激光剥蚀系统(激光波长分为 193 nm 和 213 nm 两种),MPI Mainz 实验室使用的就是这套系统,文章对此作一详细介绍。文中阐述了数据优化技术及其多种校正过程;介绍 LA - ICPMS在痕量元素和同位素分析领域的一些应用,包括参考物质的研制,Hawaiian 玄武岩、Martian 陨石、生物骨针和珊瑚虫中痕量元素分析及熔融包裹体和富钙 - 铝碳质球粒陨石中的铅和锶同位素测量。

关键词：激光剥蚀 - 等离子体质谱；地质样品；参考物质；陨石；生物样品；痕量元素；同位素比值

中图分类号：O657.63　　**文献标识码**：A

1 Introduction

Laser ablation-inductively coupled plasma mass spectrometry (LA-ICPMS) has become a powerful analytical technique used in nearly all subdisciplines of geochemical, cosmochemical and environmental research[1]. The growth of LA-ICPMS can be seen by an evaluation of recent publication history over the last decade. For example, there has been steady increase of the number of publications in the Journal of Analytical Atomic Spectrometry (JAAS) from 4 in the year 1995, to 18 in 2001 and then to 40 in 2007. A recent review[2], noted that the use of LA-ICPMS has substantially increased and it concluded that the trend will continue for the foreseeable future. Additionally, the top 20 most frequently requested reference materials of the GeoReM database (http://georem.mpch-mainz.mpg.de[3]) comprise 12 reference glasses from the National Institute of Standards and Technology (NIST), the United States of Geological Survey (USGS) and the Max-Planck-Institut für Chemie (MPI-DING) mainly used as calibration materials for LA-ICPMS and other microanalytical techniques.

2 Types of LA-ICP Mass Spectrometers

There are a variety of lasers and mass spectrometers that are used for LA-ICPMS analysis. Each of their analytical features differs and they are used for applications with various requirements, such as routine trace element, high-precision isotopic analysis, or bulk and micro analysis of geological, biological and environmental samples. The commonly used mass spectrometers and lasers are compared in Table 1 and Table 2 and explained below.

2.1 Quadrupole Mass Spectrometers

Quadrupole mass spectrometers apply voltages on four parallel metal rods affect the trajectory of ions extracted from the ICP′s plasma. Only ions of a certain mass pass through the quadrupole, which can be considered as a mass filter. Quadrupole mass spectrometers have the advantages of extremely fast scan times (e.g. 0.25 s for the determination of 25 trace elements) and are relatively small, low-cost systems. The primary disadvantages are the low mass resolution (about 300) of the quadrupole and the non-flat triangular peak shape, which does not allow for precise isotope ratio measurements.

Table 1　The commonly used ICP-MS

parameters	mass spectrometers			
	quadrupole	single collector sector-field	time-of-flight	multicollector sector-field
scan time from one mass to another	fast	electrical scan: fast, magnetic scan: slow	very fast	scanning is not usual, very slow
mass resolution	300 ~ 400	300 ~ 10000	500 ~ 2000	300
peak shape	triangular	flat top	triangular	flat top
sensitivity (cps/ppm)	medium to high	high	low	high
applications	elemental analysis	elemental and isotopic analysis	fast scanning capability	high-precision isotopic analysis

Table 2　Lasers commonly used for laser ablation

parameters	lasers				
	Nd:YAG	Nd:YAG	Nd:YAG	ArF excimer	fs laser
wavelength (nm)	266	213	193	193	196 ~ 800
pulse energy (mJ)	0.5 ~ 4	0.2 ~ 2	0.1 ~ 1	0.05 ~ 0.8	1 ~ 4
pulse width	9 ns	5 ns	3 ns	15 ns	60 ~ 400 fs
repetition rate (Hz)	1 ~ 20	1 ~ 20	1 ~ 10	1 ~ 100	1 ~ 10
crater diameter (μm)	3 ~ 80	2 ~ 160	5 ~ 100	4 ~ 200	5 ~ 100

2.2 Single-collector Sector-field Mass Spectrometers

Single-collector sector-field mass spectrometers, which contain magnetic and electric sector fields, are used for sensitive LA-ICPMS trace element analyses. The magnetic sector field separates ions according to their mass-to-charge ratio, whereas the electric sector

focuses ions according to their kinetic energy. Because of the developments of fast magnets, reasonable scan times (about 1 ~ 2 s) can be obtained for the LA-ICPMS analysis of 40 ~ 50 trace elements. The major advantage is the potential for high mass resolution (up to 10000) to separate masses of interest from disturbing molecular interferences. Most analysts, however, use the low mass resolution mode (300) that yields flat-top peaks to obtain highly sensitive elemental analyses and relatively precise isotope ratio measurements. As a trade off between resolution and sensitivity, some laboratories compromise with a mass resolution of about 4000 for their LA-ICPMS analyses, which does allow the separation of many mass lines of interest from disturbing molecule lines.

2.3 Time-of-Flight Mass Spectrometers

Time-of-flight mass spectrometers (TOF-MS) measure the mass-dependent time and it takes ions of different masses to move from the ion source to the detector. This requires that the starting time (the time at which the ions leave the ion source) is well-defined. This type of mass spectrometer is only used in some LA-ICPMS laboratories[4]. The major advantages include the fast speed of acquisition and high ion transmission. However, the dynamic range of the instruments is limited. Due to their relatively low sensitivity, TOF mass spectrometers have higher detection limits than quadrupole instruments.

2.4 Multi-collector Sector-field Mass Spectrometers

Similar to the mass spectrometers described above in chapter 2.2, multi-collector sector-field mass spectrometers consist of magnetic and electric field sectors. However, multiple collectors are used for the simultaneous measurements of ions. Because of this and the consistent mass bias variation across the mass range, highly precise isotope ratios can be obtained. Disadvantages include the low mass resolution of most instruments, which can lead to significant interferences caused by doubly charged ions, oxides and argides. Faraday cups are generally used and therefore only isotopes of high-abundant elements (e. g. > ca. 50 μg/g for Pb, > ca. 500 μg/g for Sr) can be measured with high precision. Because of the slow switching, but very stable magnets used, MC-ICPMS instruments are not suitable for multi-element analysis.

2.5 Nd:YAG Lasers

Nd:YAG lasers are widely used in LA-ICPMS laboratories. Early LA-ICPMS systems used the fundamental wavelength of 1064 nm, which is poorly absorbed by many minerals. Therefore, new developments in Nd:YAG lasers led to the use of harmonic wavelengths of 532 nm, 266 nm, 213 nm and 193 nm. With shorter wavelengths, smaller particles are produced and there is a higher absorption of the laser energy in the surface layers of materials. Like the wavelength, pulse length has a considerable influence on the quality of the results-shorter pulses increase the energy deposited in the area to be analyzed. State-of-the-art Nd:YAG lasers typically employ wavelengths of 193 nm or 213 nm and pulse lengths of 3 ~ 5 ns. Laser ablation systems using Nd:YAG lasers are relatively compact.

2.6 ArF Excimer Lasers

ArF excimer lasers have a short wavelength of 193 nm producing less severe fractionation effects because of almost complete vaporization and excitation of all ablated particles in the ICP[5]. Very flat crater shapes can be obtained using these lasers. However, the longer pulse lengths (about 15 ns) compared to the Nd:YAG lasers and the much larger size of the instruments have left this as a less-used option for LA-ICPMS.

2.7 Femtosecond (fs)-Lasers

At present, femtosecond(fs)-laser is only applied to LA-ICPMS in some laboratories[6-8]. Due to the fs time scale, ablation is essentially non-thermal. This is important for complex matrices, where the elemental fractionation is similar. A Ti sapphire laser having 800 nm and more recently 260 nm has been used in fs laser ablation studies.

3 Results and Discussions

3.1 Measurement Procedures

Different procedures have been used to convert the count rates and the voltages for the ions in element abundances and isotope ratios, respectively. It is beyond the scope of this paper to explain and to evaluate all these procedures for the different combinations of ICP mass spectrometers and laser ablation systems. The evaluation technique as used in the MPI Mainz laboratory will be elaborated as follows. In this laboratory, LA-ICPMS analyses are performed with the single-collector sector-field ICP mass spectrometer ThermoFinnigan Element 2, which is connected alternatively with the UP213 or the UP193SS Nd:YAG laser ablation system from New Wave[9]. Such combinations have also been used in many other laboratories worldwide and have delivered highly sensitive and precise trace element and isotope data. Typical instrumental parameters of the mass spectrometer and the laser ablation systems are listed in Table 3. For most measurements the low mass resolution mode (mass resolution = 300) of the ICP-MS is used. Routine trace element analyses are performed using the combination of magnetic (B scan) and electric scan (E scan) modes of the Element 2. Scan times for the determination of 40 ~ 50 trace elements are about 1.5 s. This means that

during a 1 minute analysis of a single spot, about 40 scans can be performed. For isotope analysis of Pb and Sr only the E scan mode is used allowing a quasi simultaneous determination of 1 000 ~ 2 000 scans during a 1 min ablation period.

Table 3　Typical operating parameters

parameters	New Wave laser ablation systems	
	UP 193SS	UP 213
wavelength (nm)	193	213
pulse length (ns)	2.8	5
energy density (J/cm^2)	5 ~ 6	7 ~ 10
irradiance at sample (GW/cm^2)	1.8 ~ 2.1	1.4 ~ 2.0
spot size (μm)	2 ~ 100	5 ~ 160
pulse repetition rate (used)	10	10

parameters	ThermoFinnigan Element 2	
	mass resolution = 300	mass resolution = 4000
RF power (W)	1270	1270
cool gas flow rate (L/min)	15	15
auxiliary gas flow rate (L/min)	1	1
carrier gas (Ar) flow rate (L/min)	0.8	0.8
carrier gas (He) flow rate (L/min)	0.7	0.7
sample time (s)	0.002	0.005
samples per peak	100	15
mass window (%)	10	150

To determine elemental concentrations, where the isotopes of interest may be interfered by molecules in the low mass resolution mode, a mass resolution of about 4000 (the medium resolution mode of the Element 2) has been successfully used[10]. Fig. 1 shows a typical example of a mass spectrum at mass number 32 containing an interference. The figure shows that at a resolution of 4 000, the mass of interest (^{32}S) is obviously separated from the oxide molecule ($^{16}O_2$).

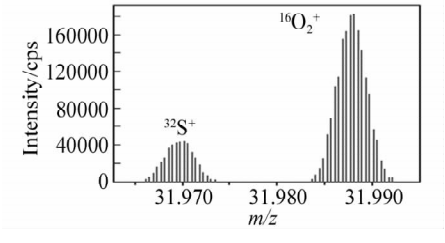

Fig. 1　Highly resolved mass spectra at mass number 32 (mass resolution = 4000)

The ^{32}S peak is obviously separated from the oxygen molecule.

3.2　Corrections

To obtain accurate and precise analytical data, raw ion intensities must be corrected. The most important corrections are discussed below.

3.2.1　Dead Time

Knowledge of the multiplier dead time is important for a precise isotope and element analysis using the counting modes, particularly when the count rates are high. The dead time (typically between 12 and 30 ns) can be determined at regular intervals using different concentrations of the NIST 982 Pb spike solution having $^{208}Pb/^{206}Pb = 1$ and $^{208}Pb/^{204}Pb = 36.75$[11]. The proprietary software then corrects ion intensities.

3.2.2　Blank

Gas blanks (generally ranging from 0 ~ 100 cps for REE, Th, U, Hf to about 1000 cps for Cs, Rb) are measured before each spot analysis and the ion intensities are accordingly corrected.

3.2.3　Interference

For routine multi-element analysis, isobaric interferences are not generally problematic in LA-ICPMS analysis, because at least one isotope is interference-free for most elements, e.g. ^{139}La, ^{140}Ce, ^{141}Pr and ^{143}Nd. For *in situ* radiogenic $^{87}Sr/^{86}Sr$ isotope measurements the isobaric interference of ^{87}Rb on ^{87}Sr must be corrected. Because of their low mass difference ($\Delta m = 0.0003$ u), ^{87}Rb and ^{87}Sr cannot be separated-even in the high mass resolution mode of the mass spectrometer (mass resolution = 10 000). The peak of mass number 87 has therefore to be corrected for ^{87}Rb using the interference-free ^{85}Rb isotope and assuming a uniform $^{87}Rb/^{85}Rb$.

For element analysis, molecule interferences are the most problematic. Oxides and other molecular ions, e.g. argides, can falsify the analytical results. However, oxides can be drastically reduced by tuning the mass spectrometer to low oxide rates (ThO/Th < 1%). In addition, we prefer non-even masses for the analysis of geological samples: oxide interferences are higher for even masses because of the even mass of ^{16}O and the high-abundances of other even isotopes, such as ^{24}Mg, ^{28}Si, ^{40}Ca and ^{56}Fe in natural samples. Matrix-matched calibration with samples having similar trace element contents and oxide production and/or use of medium mass resolution, where oxides are separated (e.g. ^{32}S from $^{16}O_2$, seen in Fig. 1), help to get reliable LA-ICPMS data.

Finally, interferences from doubly charged ions may overlap with isotopes of interest, e.g. $^{86}Sr^+$ from $^{172}Yb^{++}$. However, we have found that doubly charged ion production in the Element 2 can be minimized to negligible amounts in the ion source using the conditions

listed in Table 3. Furthermore, in most natural rock samples, elements with low Z are generally more abundant than elements with high Z. This leads to extremely low doubly charged to single charged ratios, e.g. $^{172}Yb^{++}/^{86}Sr^{+} < 0.00008$ in basalts.

3.2.4 Internal Standard

An internal standard (mainly ^{43}Ca, ^{44}Ca, ^{29}Si or ^{30}Si for the analysis of rock samples) is used to compensate for the unstable ion beam during ablation. Fig. 2 demonstrates the corresponding decrease of internal standard (^{43}Ca) and trace element count rates during a geological glass spot analysis, noting that the internal standard normalized count rates are nearly uniform. The peak of the internal standard element should be interference-free to avoid introducing systematic errors into the trace elemental analysis. As the highly resolved mass spectra of Fig. 3 show, the occurrence of $^{27}Al^{16}O$ in high-Al samples may interfer the ^{43}Ca isotope in low mass resolution. High Si samples can also interfere with ^{44}Ca as $^{28}Si^{16}O$. In this case, oxide production can lead to 1% ~ 3% higher Ca peaks for high Si/Ca (>100) and Al/Ca (>5) samples using low mass resolution, even when tuning ThO/Th < 0.5%. For example, a non-matrix- matched calibration of rhyolites (e.g. ATHO-G; Al/Ca = 5.3[12]) produces systematically lower trace element data (by several percent) when using the synthetic NIST SRM 612 or NIST SRM 610 glasses for calibration since these glasses have a low Al/Ca (0.13).

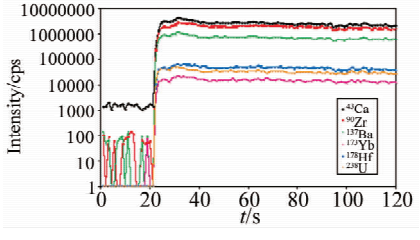

Fig. 2　Intensity of ^{43}Ca (internal standard) and trace elements during the spot analysis of the basaltic reference glass KL2-G using a 213 nm Nd:YAG laser

The run consists of about 20 s blank and 100 s ablation measurements (160 μm spot diameter, 10 Hz). Note the small (ca. 35%) and similar decrease of all isotopes; this means that the ^{43}Ca normalized count rates are nearly uniform.

3.2.5 Mass Fractionation

The quantification of isotopic and elemental ratios by LA-ICPMS is biased by mass fractionation effects caused by the variable deflection of light to heavy ions in the ICP-MS and by the different behavior of these masses during ablation. The correction for mass fractionation in routine elemental analysis occurs with the determination of relative sensitivity factors from analyses of reference materials (see below), which includes all types of mass and element fractionations. In isotopic analysis, an accurate determination of mass fractionation is essential to obtain accurate results. For Pb isotopic analysis of geological glasses, external calibration of Tl and Pb isotopes using the synthetic NIST SRM 612 glass can be used[13-15]. Matrix-dependent mass fractionation has not been observed within the limits of about a 0.1% error for single- and multi-collector LA-ICPMS. The mass fractionation of Sr isotopes was determined by internal calibration[16] using the known and constant $^{88}Sr/^{86}Sr$ for the determination of $^{87}Sr/^{86}Sr$.

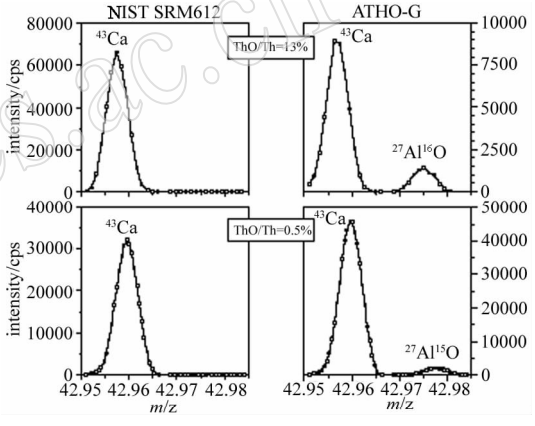

Fig. 3　^{43}Ca and $^{27}Al^{16}O$ peaks obtained from the analysis of NIST SRM 612 (Al/Ca = 0.1) and ATHO-G (Al/Ca = 5) reference glasses using a mass resolution of 4000

The spectra for two different tuning conditions (ThO/Th = 13 and 0.5%, respectively) are shown.

3.2.6 Elemental Fractionation

Elemental fractionation describes the behavior of different elements during ablation. It is extremely dependent on the elements investigated (e.g. high: Zn-Ca; low: Sr-Ca) and the laser system used (high: 266 nm laser; low: 193 nm laser, fs laser). The particle size distribution has the most important influence on elemental fractionation[17], which is a function of laser wavelength. Smaller mean particle sizes were obtained with decreasing wavelengths in the order 1 064 nm > 532 nm > 266 nm > 213 nm > 193 nm. The fractionation factor[18] is a measure of the element fractionation and is calculated by dividing the total counts of the second half of the single-spot

analysis by the counts of the first half and normalized to the internal standard. Whereas the fractionation factors for lithophile elements (e.g. Sr, Ba, REE) are about 1 (no fractionation) using Ca as internal standard, they can exceed up to 2.5 for chalcophiles (e.g. Pb, Zn, S) and siderophiles (e.g. Re, Ni, W) using 266 nm Nd:YAG lasers[1]. Spot analyses using modern 213 nm and 193 nm Nd:YAG lasers yield minimal fractionation factors (<1.05), even for Pb and the volatile elements Rb and Cs[9].

3.2.7 Element Sensitivity

Elements are ionized to different degrees, and ionization energy of the element is one of the most important parameters for this process. Whereas elements with relatively low (<5 eV) first ionization energies (e.g. alkalis) are nearly completed ionized in the plasma torch, the degree of ionization of noble metals and halogens with first ionization energies >9 eV is poor. Here, a relative sensitivity factor, RSF, is used to calibrate the variable ionization behavior of the elements. It is defined as $RSF = c_{uncorr}/c_{true}$, where c_{uncorr} is the uncorrected concentration of an element obtained by LA-ICPMS and c_{true} is the "true" concentration. RSFs are generally determined from the analyses of reference materials; most LA-ICPMS analysts use the well-known NIST SRM 610, SRM 612, USGS BCR-2G and/or MPI-DING KL2-G glasses to generate an ionization correction factor for geological samples. Fig.4 shows the RSFs obtained in the Mainz laboratory for the synthetic SRM 612 and the geological KL2-G glasses. The RSFs of some elements (e.g. Cu, Rb, Pb) differ significantly by about 5% ~10% for the two glasses. This means that for highly accurate analyses, a matrix-matched calibration should be used. The use of fs lasers will certainly help to overcome matrix problems in LA-ICPMS.

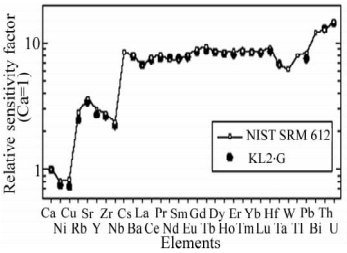

Fig. 4　Relative sensitivity factors obtained from the analyses of the synthetic NIST SRM 612 and the basaltic KL2-G glasses using the UP 213 laser ablation system

The data for most elements agree within analytical uncertainties of 1% ~5%. However, there are significant differences for some elements (e.g. Cu, Rb, Pb) due to matrix effects.

3.3 Calibration Materials

The accuracy of LA-ICPMS data is primarily dependent on calibration techniques. Without reference materials it is difficult to produce reliable data sets and certified geological reference glasses are most useful for a matrix-matched calibration of rock and mineral samples. At present, there are 17 synthetic and geological glasses and 18 mineral samples, which were used worldwide in LA-ICPMS laboratories[19]. The most important reference materials that we use in our laboratory are:

NIST SRM 610 and SRM 612: These glasses were used as calibration materials for a variety of samples in LA-ICPMS. It has been shown by many authors that these glasses are homogeneous for many elements with respect to LA-ICPMS analysis. Advantages of these samples are the high trace element contents of about 400 (NIST SRM 610) and 40 μg/g (NIST SRM 612). Drawbacks are that only 8 elements have been certified by NIST and the matrix is quite different from any geological matrix. However, reasonably good compilation data of Pearce et al.[20] and of the GeoReM database are available and systematic errors caused by non-matrix matched calibration may be less than 10% using 193 nm and 213 nm lasers.

USGS BCR-2G, BHVO-2G, BIR-1G: To overcome non-matrix matched calibrations, the USGS has prepared a set of geological (basaltic) reference glasses. These samples have natural element patterns and are therefore very useful as quality control materials. The low contents of some trace elements are not suitable for a precise primary calibration. No certified reference values are available; however, the compilation values of the USGS and the GeoReM database have a high degree of confidence.

MPI-DING KL2-G, ML3B-G, StHs6/80-G, ATHO-G, T1-G, GOR128-G, GOR132-G, BM90/21-G: The Max-Planck-Institut für Chemie has prepared a set of eight reference glasses of different natural (basaltic, andesitic, rhyolitic, quartz-dioritic, komatiitic, peridotitic) composition. They have been certified[12] using the IAG protocol for certification[21]. About 50 reference and 25 information values are available for each MPI-DING glass. In addition, data for the isotopic compositions of 12 elements (H, O, Li, B, Si, Ca, Sr, Nd, Hf, Pb, Th, U) exist. As for BCR-2G, BHVO-2G and BIR-1G, these reference glasses are valuable samples for quality control and also with some limitations for use as calibration

materials[9] for quite different geological matrices.

USGS GSC-1G, GSD-1G, GSE-1G: This set of synthetic USGS reference glasses has basaltic major element compositions and is therefore especially suited for LA-ICPMS calibration of basaltic geological samples. Similar to the NIST glasses the USGS GS glasses contain uniform trace element concentrations at about 5 μg/g, 50 μg/g and 500 μg/g. Until now they have been not certified. However, high-precise isotope dilution, ICP-MS and LA-ICPMS data for these glasses exist, which are mostly consistent[22-23]. GeoReM preferred values therefore have a high degree of confidence.

3.4 Uncertainties

3.4.1 Concentrations

To verify the quantitative reproducibility of our LA-ICPMS technique we analyzed homogeneous glasses at different times. As an example, Fig. 5 shows the Sr concentrations in the KL2-G glass, which were obtained from different independent analyses performed during a period of several months. Each three-spot analysis has an internal precision (1RSE, relative standard error) of better than 1% using spot sizes of 120 μm. This value is typical also for other elements having concentrations higher than about 1 μg/g. Lower abundances in the ng/g range yield RSE values of 1% ~5%. The external precision defined as 1RSD (relative standard deviation) is lower; the results of the 10 Sr analyses shown in Fig. 5 yield an external precision of 3%. LA-ICPMS measurements done in the medium mass resolution mode are less precise because of lower count rates and non-flat peak shapes. Table 4 shows that an internal and external precision of about 5% can be obtained for concentrations >10 ~20 μg/g. Analyses performed with lower crater sizes yield less precise data. However, as the data of the Beijing laboratory show (Table 5), precision is about 5% using crater sizes of 40 μm.

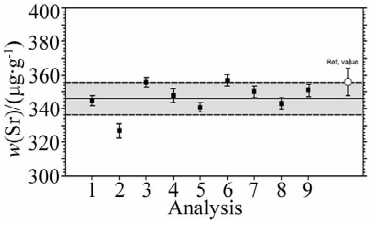

Fig. 5　Sr concentrations obtained from 9 independent LA-ICPMS analyses of the KL2-G reference glass

The analyses were performed within 7 months. Error bars give the uncertainty (± 1SE) of a single analysis. External precision (1 RSD) is 3%. The reference value[12] (with uncertainty at 95% confidence level) is also shown.

Table 4　Concentration data of components in two bottles of BRP-1①

components	Bottle A		Bottle B		reference value	*U*
	concentration	SD	concentration	SD		
MgO	3.87	0.08	3.92	0.06	3.94	0.03
Al_2O_3	12.6	0.5	12.2	0.1	12.4	0.1
TiO_2	3.76	0.06	3.78	0.11	3.81	0.03
FeO	13.6	0.1	13.9	0.2	14.0	0.1
Sc	26	1	28.2	0.5	28.5	0.8
V	387	14	389	7	391	7
Cr	9.9	0.6	7.6	0.6	12.4	1.0
Mn	1660	40	1660	30	1660	20
Co	36.7	0.9	37.3	1.0	37.5	1.4
Ni	22.1	0.6	23.1	1.5	23.4	0.9
Cu	150	9			160	3
Zn	143	32			142.2	1.8

① The LA-ICPMS data were obtained by using a mass resolution of 4000. They are compared with certified reference values[24]. SD: standard deviation, U: uncertainty at 95% confidence level. Concentration unit: % (mass ratio) for major elements, μg/g for other elements.

Table 5　Trace element concentrations (μg/g) in the ML3B-G reference glass determined in two different LA-ICPMS laboratories using spot sizes of 120 μm (Mainz) and 40 μm (Beijing), respectively①

elements	reference value[12]		LA-ICPMS lab (Mainz)[12]			LA-ICPMS lab (Bejing)		
	concen.	95% CL	concen.	SD	RSD/%	concen.	SD	RSD/%
Co	41.2	3.5	41.8	0.1	0.2	44.1	1.1	2.4
Ni	107	9	98.8	1.3	1.3	115	1	1.3
Cu	112	10	112	1	0.6	119	1	0.8
Ga	19.6	2.1	18.9	0.1	0.5	20.0	0.3	1.6
Rb	5.80	0.21	5.61	0.03	0.5	5.82	0.12	2.1
Sr	312	4	312	3	1.1	332	10	3.0
Y	23.9	0.7	24.8	0.2	0.8	24.1	0.7	2.8
Zr	122	3	122	1	0.9	119	5	4.4
Nb	8.61	0.22	8.54	0.07	0.8	8.77	0.31	3.5
Cs	0.140	0.012	0.15	0.03	21	0.13	0.02	15
Ba	80.1	2.2	77.7	0.2	0.3	81.4	2.6	3.2
La	8.99	0.13	9.45	0.13	1.4	9.67	0.19	1.9
Ce	23.1	0.3	22.6	0.2	1	25.4	0.6	2.5
Pr	3.43	0.06	3.45	0.03	0.9	3.65	0.17	4.6
Nd	16.7	0.2	17.1	0.2	1.3	18.5	0.6	3.2
Sm	4.75	0.07	4.85	0.02	0.5	5.31	0.28	5.2
Eu	1.67	0.02	1.72	0.003	0.2	1.75	0.10	6.0
Gd	5.26	0.23	5.25	0.14	2.6	5.55	0.54	9.7
Tb	0.797	0.021	0.83	0.01	0.8	0.79	0.05	6.1
Dy	4.84	0.07	5.07	0.09	1.7	4.87	0.10	2.1
Ho	0.906	0.018	0.96	0.01	0.6	0.90	0.03	3.2
Er	2.44	0.05	2.50	0.03	1.2	2.32	0.07	3.2
Tm	0.324	0.007	0.33	0.01	3.7	0.36	0.03	9.4
Yb	2.06	0.04	2.14	0.10	4.6	2.34	0.17	7.2
Lu	0.286	0.006	0.30	0.01	3.2	0.31	0.02	7.9
Hf	3.22	0.08	3.40	0.02	0.7	3.29	0.09	2.8
Ta	0.555	0.013	0.52	0.02	4.5	0.56	0.05	8.1
Pb	1.38	0.07	1.32	0.04	2.7	1.19	0.09	7.9
Th	0.548	0.011	0.56	0.004	0.8	0.59	0.05	7.9
U	0.442	0.018	0.50	0.004	0.8	0.41	0.06	14

① 95% CL: Uncertainty at 95% confidence level; SD: standard deviation; RSD: relative standard deviation in percent; concen.: concentration.

Uncertainties at 95% confidence level include all sources of uncertainties, such as statistical errors of measurements from the sample and the reference material, uncertainties from the calibration procedures[9]. Calculated relative uncertainties at 95% confidence level are 3% ~ 10% for concentrations >1 μg/g using spot sizes of 120 μm, when accurate reference values of the calibration materials (about 1% ~2%) are available and matrix-matched calibration can be performed. The accuracy is demonstrated in Fig. 6, where the mean deviation of the MPI Mainz data from the certified values[10] is about 4% for the ML3B-G reference glass. For 40 μm spot size measurements a mean deviation of 6% was obtained from the Beijing laboratory.

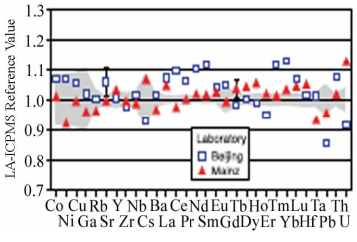

Fig. 6　Trace element data for the ML3B-G reference glass obtained in two different LA-ICPMS laboratories

They are normalized to the reference values[12]. The shaded field represents the uncertainties of the reference values. The bars indicate typical uncertainties (1 SD) for the LA-ICPMS data using spot sizes of 120 μm (Mainz) and 40 μm (Beijing), respectively.

3.4.2　Isotope Ratios

Extensive studies of Pb and Sr isotope ratio measurements with the singe-collector sector-field ICP-MS Element 2 have been performed in our laboratory[13-14,16]. Fig. 7 shows the precision we obtained for Pb isotope ratios in the MPI-DING reference glasses having Pb of 2 and 5 μg/g, respectively. RSD values are dependent on the laser system used, the Pb concentration of the sample and the spot size used. An external precision of better than 0.2 and 0.1% can be obtained for $^{208}Pb/^{206}Pb$ and $^{207}Pb/^{206}Pb$ using the 213 nm and the 193 nm Nd: YAG lasers, respectively[16]. Single-collector sector-field mass spectrometers, such as the Element 2, are especially useful for Pb isotope analysis of low-Pb samples (about 0.1 ~ 20 μg/g; e.g. melt inclusions) using relatively large spot sizes of 60 ~ 120 μm or for highly resolved microanalyses of high-Pb samples (> 300 μg/g; e.g. manganese crust) using small spot sizes of 5 ~ 10 μm. *In situ* LA-ICPMS measurements of $^{87}Sr/^{86}Sr$ in low-Sr samples (30 ~ 300 μg/g) have been recently performed using the Element 2 ICP-MS[16]. Various corrections have to be made for the determination of $^{87}Sr/^{86}Sr$: dead time correction of the ion counting system, blank, isobaric interference of Kr (about 2% if ^{86}Sr = 30 μg/g), possible interferences from doubly charged REE and Hf, isobaric interference of ^{87}Rb on ^{87}Sr (should not exceed 30% or Rb/Sr = 0.1 for precise analysis), mass bias correction for ^{87}Sr using ^{88}Sr and the corrected ^{86}Sr, final correction for $^{87}Sr/^{86}Sr$ (caused by unknown mass discrimination for Rb) using well-documented reference glasses (e.g. KL2-G, ML3B-G and BHVO-2G) with known $^{87}Sr/^{86}Sr$ and similar matrix. First results on reference glasses show that an external precision of about 0.03% RSD can be obtained using the 193 nm Nd: YAG laser for sample ablation (Fig. 8).

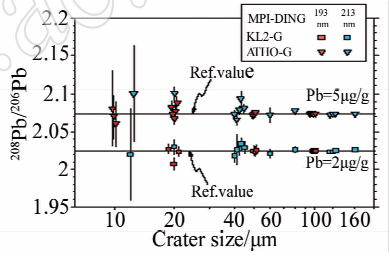

Fig. 7　$^{208}Pb/^{206}Pb$ ratios obtained from sets of three-spot analyses using different spot sizes and two different Nd: YAG lasers

Error bars indicate ± 1SE (n = 3). The data are compared with reference values from TIMS and MC-ICPMS analyses[12].

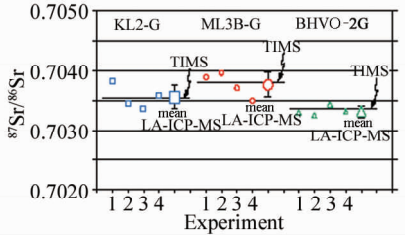

Fig. 8　$^{87}Sr/^{86}Sr$ ratios obtained from 4 sets of three-spot LA-ICPMS analyses of basaltic Hawaiian reference glasses using a 193 nm Nd:YAG laser and a spot size of 50 μm

Error bars indicate external precision (1RSD). The data are compared with high-precision TIMS data[12].

3.5　Detection Limits

LA-ICPMS ranks among the most sensitive analytical techniques for trace element analysis. The

limit of detection (LOD) of an element, defined as $3\sigma_B$, where σ_B is the standard deviation of readings on the blank, is dependent on several factors, where the most important are its individual element sensitivity, the isotopic abundance, the sample amount ablated per time (this means large crater sizes, repetition rates and laser energies improve detection limits), the measuring time and the gas blank (long measuring times and low gas blanks improve detection limits) and the sample. Fig. 9 shows our results for a glass using 120 μm spot size. LOD vary between 0.000 1 and 0.1 μg/g. They decrease with increasing atomic number. The concentrations of most trace elements in rock samples (e.g. oceanic island basalt BHVO-1) are three orders of magnitude higher than the LOD.

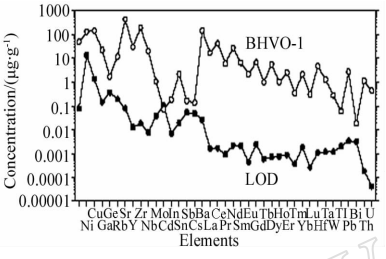

Fig. 9　Limits of detection (LOD) for LA-ICPMS using 120 μm spot size

For comparison, the concentrations in a typical oceanic island basalt (BHVO-1) are also plotted.

4　Applications

LA-ICPMS has been used in the MPI laboratory for a wide variety of different applications. In the following sections, some examples from the fields of geochemistry, cosmochemistry and environmental research will be given.

4.1　Trace Elements in Reference Glasses

LA-ICPMS is useful to investigate trace elements in a variety of glass samples. Homogeneity tests have been performed for the geological MPI-DING and USGS GS reference glasses[12, 22-23]. The LA-ICPMS data (Fig. 10) indicate that most elements are homogeneously distributed in these reference glasses. This is especially true for the lithophile elements, such as Sr, Nb, Nd and U. Some chalcophile and siderophile elements (e.g. Cu, Sn and Bi) show small heterogeneities.

Reference glasses have been used as calibration materials in different fields of research. Table 6 lists some trace element data, which we obtained for the synthetic geological USGS glasses GSC-1G, GSD-1G (used in geochemistry) and the two well-characterized float glasses FGS-1 and FGS-2 from the Bundeskriminalamt (BKA/Federal Criminal Police Office), Germany (used in forensics). Nearly all LA-ICPMS data agree within uncertainty limits with consensus values[25].

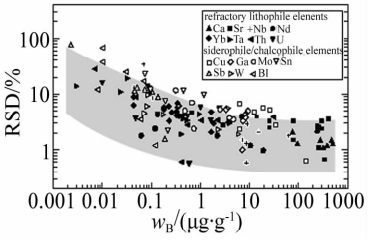

Fig. 10　Concentrations and relative standard deviations (RSD) for elements obtained from spot analyses on different locations of the MPI-DING glasses[12]

Most elements lie within the (shaded) repeatability field of LA-ICPMS, indicating that possible chemical heterogeneities are smaller than the uncertainty of LA-ICPMS. Possible micro-heterogeneities are found for Cu, Sn and Bi.

4.2　Fused Rock Reference Materials

Most rock reference materials are powdered samples. However, pressed pellets are not suitable for precise LA-ICPMS analysis, because different rock types have different mineral sites for particular trace elements that may be sampled to different degrees by laser ablation. Therefore, Fedorowich et al.[26] experimented with flux-free fusions of rock powders using a tungsten strip heater cell. In our laboratory, Stoll et al.[27] have developed an automated iridium-strip heater to produce small amounts (10 ~ 100 mg) of homogeneous glasses from rock powders. These investigations demonstrated that the fused glasses were homogeneous with respect to major and trace elements, and were not depleted in elements with condensation temperatures > 900 K (e.g. Zr, Hf, Ba, Th, U, rare earth elements, Y, Sr and Rb) using a melting temperature of 1 600 ℃ and a melting time of 10 s. The new basaltic reference material BRP-1[28] was prepared using these melting conditions and subsequently analyzed. Table 4 shows some new trace element data obtained using highly resolved mass spectra at a mass resolution of 4 000[10]. Most data agree with the certified values[24] within uncertainty limits.

Table 6　Trace element data for the geological USGS glasses GSD-1G, GSC-1G and the forensic BKA glasses FGS 1 and FGS 2①

elements	GSD-1G		GSC-1G		FGS 1		FGS 2	
	LA-ICPMS	GPV	LA-ICPMS	GPV	LA-ICPMS	cons. val	LA-ICPMS	cons. val.
Rb	38.4 ±0.3	37.3 ±0.4	5.0 ±0.1	4.92 ±0.05	8.3 ±0.3	8.6 ±0.5	41 ±2	35 ±3
Sr	70.1 ±0.5	69.4 ±0.7	34 ±1	32.3 ±0.03	60 ±2	57 ±4	261 ±5	253 ±13
Zr	42 ±2	42 ±2	7.5 ±0.1	6.8 ±0.7	49 ±2	49 ±3	216 ±15	223 ±15
Sn		29 ±6		5.3 ±0.8	19.3 ±0.4	19 ±3	92 ±5	94 ±12
Ba	69 ±1	67 ±1	35.0 ±0.1	34.8 ±0.4	44 ±1	40 ±3	210 ±11	199 ±15
La	38 ±1	39.1 ±0.4	4.6 ±0.1	4.36 ±0.04	4.4 ±0.2	4.3 ±0.5	18.6 ±0.8	18 ±1
Ce	40 ±1	41.4 ±0.4	4.6 ±0.1	4.62 ±0.05	5.3 ±0.2	5.2 ±0.5	25 ±1	23 ±2
Nd	44 ±1	44.7 ±0.5	5.0 ±0.1	4.72 ±0.05	5.4 ±0.2	5.1 ±0.5	25.6 ±0.8	25 ±2
Hf	38 ±2	39 ±2	5.0 ±0.1	4.3 ±0.4	3.1 ±0.1	3.2 ±0.3	13.9 ±0.6	15 ±1
Pb	51.6 ±0.6	50 ±2	14.9 ±0.3	14 ±1	5.6 ±0.1	5.8 ±1.0	28 ±2	24 ±2

① LA – ICPMS results of GSD-1G and GSC-1G are cited [9]; GPV: GeoReM preferred values (http://georem.mpch-mainz.gwdg.de); cons. val.: consensus values[25]. Data unit: μg/g.

4.3　Whole Rock Analyses of Hawaiian Basalts

The Hawaii Scientific Drilling Project (HSDP) provides the opportunity to study the evolution of the Mauna Loa (ML) and Mauna Kea (MK) volcanoes over a significant portion of their lifetime[29]. We analyzed trace elements in selected whole-rock samples and natural glasses by LA-ICPMS, down to the maximum depth achieved of about 3000 mbsl (m below sea level).

4.3.1　Fused Glasses

Whole-rock powders of selected locations of the borehole were fused using the Ir-strip heater method[27] and subsequently analyzed. Fig. 11 shows the primitive-mantle normalized trace element patterns of three characteristic sample types: ML tholeiites (samples from a depth of 0 ~ 280 mbsl), MK tholeiites (depth > 340 mbsl) and MK alkali basalts overlying the Mauna Kea tholeiites (depth of 280 ~ 340 mbsl). Most elemental concentrations were determined at a mass resolution of 300; the abundances of Ti, Cu and Sc, where the lines of interest are disturbed by molecules in low mass resolution, were determined using a mass resolution of 4000[10]. Because of their lower degree of melting, alkali basalts have higher abundances of incompatible elements than tholeiites. The element patterns of Fig. 11 are characterized by a small positive Sr anomaly, especially for ML samples, and negative Th-U anomalies. Sr/Nd ratios are significantly higher in ML (18) than in MK (16) basalts, whereas ML tholeiites have lower U/La (0.018) than MK (0.022) tholeiites and alkali basalts. These measurements confirm the hypothesis[30] that the Hawaiian source contains significant amounts of recycled oceanic gabbros, which are characterized by large positive Sr anomalies and large negative Th-U anomalies.

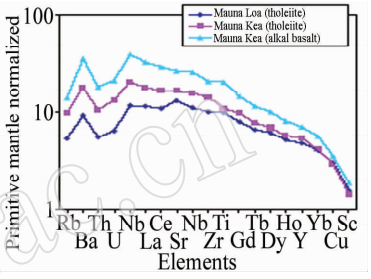

Fig. 11　Primitive mantle normalized concentrations of basalts from Mauna Loa and Mauna Kea, Hawaii

4.3.2　Natural Glasses

In order to investigate the evolution of the submarine section of the HSDP2, Amini[31] prepared 200 ~ 500 μm large hand-picked glass fragments of samples coming from a depth interval from 1314 to 3060 mbsl. In sub-samples of the same glass fragment the LA-ICPMS results are indistinguishable at each spot implying a homogeneous distribution of trace elements and Pb isotopes. The quantity of Pb measured for one three spot analysis was about 3 pg for a Pb concentration of 1 μg/g. An external precision of the Pb isotope data of about 0.2% ~ 0.3% was obtained. Fig. 12 shows the $^{208}Pb/^{206}Pb$ ratios along the stratigraphic column of the HSDP2-core. The ratios vary between 2.047 and 2.082. The lowest values are found in samples coming from depths around 1400, 2800, and 3000 mbsl whereas the highest ratios are measured in samples of 2100 mbsl depth. These data agree with high-precision TIMS data using aliquots of about 50 mg[13]. Both data sets confirm the temporal Pb isotope variations found in the HSDP-2 core based on whole-rock TIMS data[32]. Attributing

varying isotope ratios to source heterogeneities can be confirmed when considering trace element ratios. This is best demonstrated by the correlation of the element ratio of Th and U (determined by spark source mass spectrometry[31]), parent nuclides of ^{208}Pb and ^{206}Pb, with the $^{208}Pb/^{206}Pb$ ratios measured in the same glass fragments.

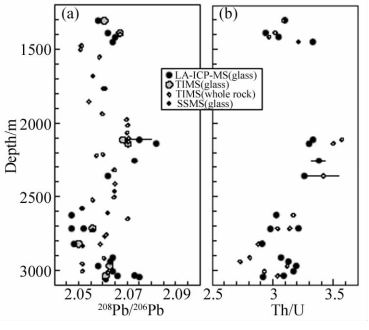

Fig. 12　$^{208}Pb/^{206}Pb$ (a) and Th/U (b) variations along the stratigraphic column of the Hawaii Scientific Drilling Project-2 drill core

LA-ICPMS, SSMS, TIMS glass data are from[13, 31]; TIMS whole rock data are from[32].

4.4　Sr and Pb Isotopes in Hawaiian Melt Inclusions

Pb and Sr isotopes of olivine-hosted glassy melt inclusions (Fig. 13) of one young (around 750 years) Mauna Loa (Puu Wahi) basalt have been investigated. Inclusions in this single sample show a large range in trace element contents similar to the entire range known for Mauna Loa[33]. The $^{208}Pb/^{206}Pb$ (2.03 ~ 2.11) and $^{207}Pb/^{206}Pb$ (0.815 ~ 0.865) ratios show large and systematic variations (Fig. 14). $^{87}Sr/^{86}Sr$ ratios are extremely heterogeneous (0.702 ~ 0.708), which can be explained by mixing of different mantle components. One of these components has high $^{87}Sr/^{86}Sr$ and low $^{208}Pb/^{206}Pb$, $^{207}Pb/^{206}Pb$ ratios, which is found in most incompatible ultra-depleted inclusions (Sr about 60 μg/g, Pb about 0.1 μg/g).

4.5　Mineral Analyses from Mantle Xenoliths

Ionov et al.[34] analyzed minerals from mantle xenoliths by LA-ICPMS in our laboratory. Fig. 15 shows the primitive mantle normalized concentrations for garnet, clinopyroxene and orthopyroxene in a garnet peridotite xenolith from central Asia. The same mineral samples were also analyzed by solution ICP-MS[35] using 10 ~ 20 mg acid-leached separates. The abundances of all trace elements in clinopyroxene by solution and laser ablation ICP-MS are close to each other. In contrast, the LA-ICPMS data for the low-abundance trace elements Th, U, Nb, La in orthopyroxene are significantly lower than those determined by solution ICP-MS. A possible reason for this is that fluid or mineral inclusions in the samples can be identified and discarded in LA-ICPMS whereas analyses of mineral separates include all impurities.

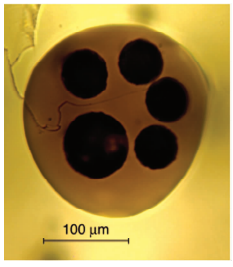

Fig. 13　Laser craters drilled in an olivine-hosted glassy melt inclusion of a Mauna Loa (Puu Wahi) basalt for trace element and isotope analysis

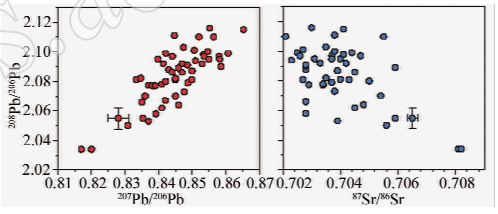

Fig. 14　*In-situ* Pb and Sr isotope ratios of Mauna Loa melt inclusions

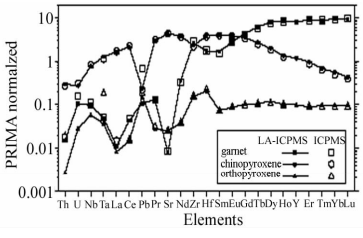

Fig. 15　Primitive mantle (PRIMA) normalized concentrations of minerals from a garnet peridotite xenolith from central Asia[34]

The LA-ICPMS data are compared with solution ICP-MS data[35].
The elements are arranged according to their degree of incompatibility.

4.6　Manganese Crust

The most extensive deposition of manganese occurs in the oceans as Fe-Mn nodules and crusts. Manganese nodules and crusts grow slowly (a few mm per million year) by direct precipitation of Mn and Fe hydroxides from ambient seawater and thus can provide

a record of changes in seawater composition through time induced by modifications in the input sources to the oceans. Changes in the erosional inputs are driven by climate changes and tectonics, which ultimately modified ocean and atmosphere circulation patterns.

The isotopic composition of Pb in manganese nodules and crusts is influenced by continental weathering (continents are uranium-rich), hydrothermal and volcanic activity at mid-ocean spreading centers (mantle is uranium-poor). Thus lead isotopes as well as trace elements can be used to fingerprint the sources and origin of material delivered to the oceans.

High-resolution records of temporal variations in seawater elemental and isotopic compositions can be obtained with LA-ICPMS. Extremely small spot sizes (Fig. 16), between 2 and 20 μm, corresponding to a time resolution of only a few thousand years provide high quality Pb isotope and trace element data, allowing to reconstruct seawater variations at glacial-interglacial time scales. Our data on a Pacific manganese crust show a secular variation in $^{208}Pb/^{206}Pb$ isotope ratios (Fig. 17), which are correlated with trace element ratios. The combined trace element and Pb isotope measurements indicate that there have been pulses of hydrothermal activity during the growth of this Mn-crust reflected in distinct signatures compared with those of the hydrogenous phases of growth.

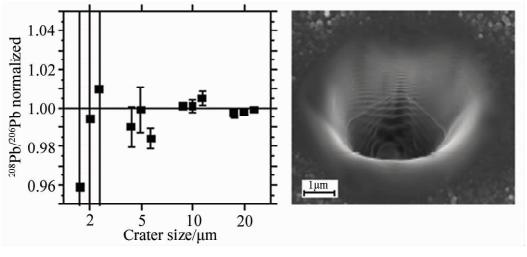

Fig. 16　Pb isotopes obtained from sets of three-spot analyses of the GSE-1G reference glass (Pb = 378 μg/g) using a 193 nm Nd: YAG laser and small spot sizes between 2 and 20 μm

Error bars indicate ± 1 SE (n = 3). 2 μm data have an internal precision of about ± 0.1. The data are normalized to the mean of the 10 μm and 20 μm data.

4.7　Martian Meteorites

In order to investigate trace element fractionation on Mars[36], we analyzed rock powders of Martian meteorites, especially the basaltic shergottites, using fused glass beads. Sample amounts used were only 10 ~40 mg. Fig. 18 shows the CI-chondrite normalized abundances of the Martian meteorite EETA 79001A[27]. Most LA-ICPMS data agree within error limits with SSMS and MIC-SSMS results obtained in the same laboratory[36] and literature data. Concentration data of some elements that are outside of the analytical uncertainties of the techniques used are presumably caused by heterogeneities of the meteorite samples.

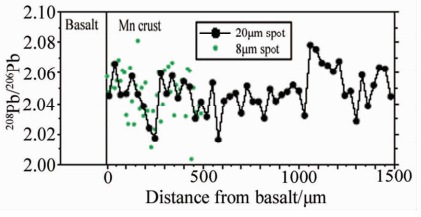

Fig. 17　$^{208}Pb/^{206}Pb$ variations in a manganese crust sample (Tunes 06 D23)

The small spot sizes correspond to a time resolution of a few thousands years.

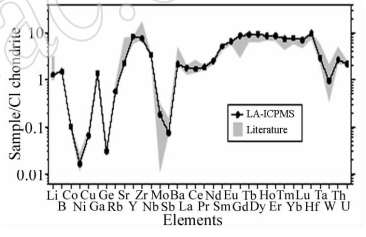

Fig. 18　CI chondrite normalized trace elements of the Martian meteorite EETA 79001A

The LA-ICPMS data are compared with literature values.

4.8　Ca-Al rich Inclusions in Stony Meteorites

It is generally believed that Ca, Al-rich inclusions (CAIs) of carbonaceous chondrites formed very early in the solar nebula by high temperature processes[37]. Lead isotopes contain a record of the chemical environment in which the Pb resided via their uranogenic and thorogenic Pb components. We used LA-ICPMS to determine $^{208}Pb/^{206}$ Pb, $^{207}Pb/^{206}$ Pb ratios, and Pb, Th, U abundances in CAIs and matrix from some carbonaceous chondrites (Fig. 19)[38].

The Pb isotopic compositions of the matrix ($^{208}Pb/^{206}Pb = 3.1$, $^{207}Pb/^{206}Pb = 1.1$) from the various chondrites are almost primordial. In contrast, 175 CAI measurements show extremely variable Pb isotope ratios: $^{207}Pb/^{206}Pb$ and $^{208}Pb/^{206}Pb$ ratios range from about 1 to 0.63, and 0.6 to 4.1, respectively (Fig. 20). Measured Pb/U and Th/U ratios are also quite variable. Th/U ratios in Allende CAIs vary from about 3 to 15 whereas

the matrix value is 3.75 ±0.11. Assuming a single-stage model and an age of CAIs of 4560 Ma, the $\mu(^{238}U/^{204}Pb)$ and $\kappa(^{232}Th/^{238}U)$ values lie between about 2 ~ 300, and 3 ~ 18, respectively. Similarly, measured versus calculated U/Pb and Th/U ratios are well correlated for the individual CAI spot analyses, showing that the Th-U-Pb system has not been significantly disturbed at about 100 μm scale.

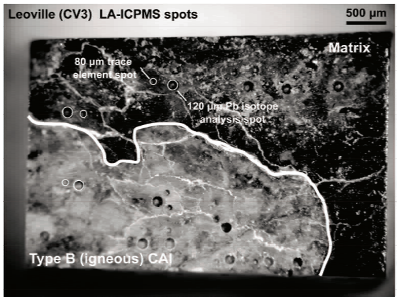

Fig. 19　Reflected light image of a portion of the Leoville (CV3) carbonaceous chondrite containing a large Calcium- Aluminum-rich Inclusion (CAI)

The sample was analyzed by LA-ICPMS and the resulting ablation craters can be seen in several locations. Outlines of selected crater locations and a demarcation of the CAI from the carbonaceous chondrite matrix have been added to the image. LA-ICPMS allows location-specific analyses for both trace element and isotope ratio quantification.

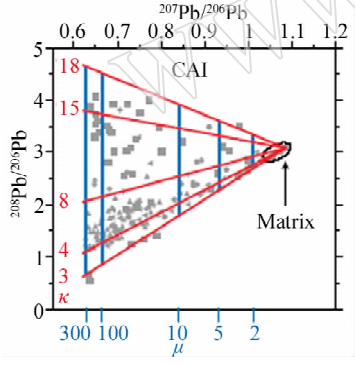

Fig. 20　Pb isotope data in CAIs of carbonaceous chondrites

Assuming a single-stage model and an age of CAIs of 4 560 Ma, the $\mu(=^{238}U/^{204}Pb)$ and $\kappa(=^{232}Th/^{238}U)$ values can be calculated.

4.9　Glass Sponges

Sponges are simple and evolutionary, among the oldest animals, first appearing ~ 800 million years ago. We have determined trace element concentrations in giant spicules (skeletal structures) of deep sea sponges (*Monorhaphis intermedia*) using LA-ICPMS[39]. The spicule, Q-B, was collected from the East China Sea and provided by the Marine Biological Museum of the Chinese Academy of Sciences, Qingdao, P. R. China. It is about 170 cm long and has a diameter of 7 mm in maximum. A complete series of LA-ICPMS analyses could be performed on the same spicule within 40 ~ 120 μm of one another (Fig. 21). The detection limits range between 0.3 and 10 ng/g. The results demonstrate that most trace elements are uniformly distributed from the axial canal to the surface of the spicule (Fig. 22).

Fig. 21　Polished cross section through a giant spicule of a deep sea sponge (*Monorhaphis*) showing the lamellar structure

Laser craters (40 μm, 120 μm) were drilled for trace element analysis.

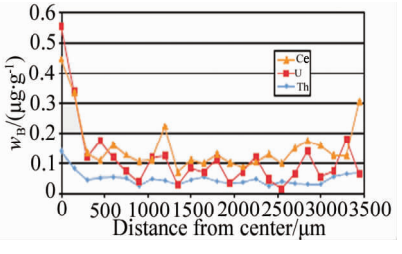

Fig. 22　Distribution of selected trace elements along the cross axis of a giant spicule

The element concentrations have been determined in 120 μm areas.

It is of prime interest that the giant spicules are composed to over 99.5% of pure silica. Na = 1500 μg/g and Ca = 200 μg/g are the most abundant trace elements in the spicule Q-B, whereas the 35 remaining elements contribute only unimportantly to the inorganic composition in bio-silica. This implies that the quality of bio-silica in the spicule is in the range of quartz grade. Amazingly, the LA-ICPMS data demonstrate that sponges produce almost pure bio-silica in an aqueous environment, which contains only trace levels of Si. These results can be explained by the ability of sponges to produce amorphous quartz glass as the material to construct their bio-silica skeleton by the enzyme silicatein. JP

4.10 Corals

Ratios of trace elements in corals, such as Sr/Ca, U/Ca, or Ba/Ca are suitable proxies for monitoring environmental conditions like sea surface temperatures (SST) or recording geological phenomena such as soil erosion or river runoff. Modern and geologically old corals can be used as archives for environmental reconstructions provided that they are not affected by diagenesis. Trace element concentrations of well-preserved *Porites* corals of Late Miocene age (ca. 9 Ma) from Crete, Eastern Mediterranean, were measured using spot sizes of 120 μm at a spatial resolution of 500 μm along the axis of maximum growth (Fig. 23)[40], corresponding to eight to eleven samples per year.

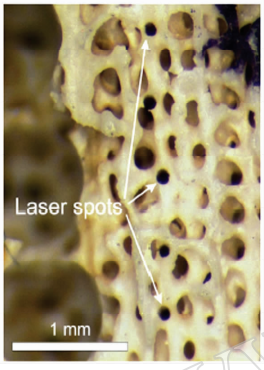

Fig. 23 Laser craters on a *Porites* coral from Crete, Eastern Mediterranean

Lattice-bound Sr and U co-vary with temperature-dependent $\delta^{18}O$ measured during previous studies[41], and thus closely reflect seasonal SST variations. The distribution of elements such as Al, Zn and Mn does not correlate with Sr or SST, but show rhythmical peaks associated with the winter months (Fig. 24). This pattern may be interpreted to represent seasonal terrigenous input into the reef environment.

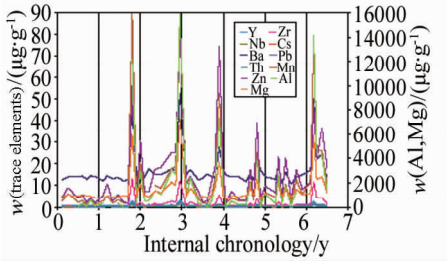

Fig. 24 Trace element distributions of a Porites coral from Crete show rhythmical peaks associated with the winter months[40]

4.11 Zircon Dating

U-Pb geochronology is based on the natural decay of ^{238}U and ^{235}U to stable ^{206}Pb and ^{207}Pb with half lives of 4.468 billion years and 0.704 billion years, respectively. The mineral most commonly used to date rocks is zircon, because it incorporates U in its structure, but accepts very little or no Pb at the time of crystallization.

LA-ICPMS and LA-multi-collector-ICPMS are capable to determine U-Pb zircon ages with reasonable accuracy and precision which has been demonstrated by a number of laboratories over the past decades. The advantages of this method are the short analytical time, moderate spatial resolution, and relatively low cost, allowing it to be useful for detrital zircon work. In our laboratory zircon dating has not been applied until now. However, Chang et al.[42] used the same configuration of instruments as in Mainz (Element 2 ICP-MS, New Wave UP213 laser) to determine zircon ages in samples previously analyzed by TIMS and/or SHRIMP, whereas ages of the samples range from ca. 56 to 1780 Ma. The authors found that the ages determined by LA-ICPMS agree well with the TIMS ages. As expected, the precision and accuracy of the $^{206}Pb/^{238}U$ and $^{207}Pb/^{206}Pb$ ages vary with the age and character of the different samples. Chang et al.[42] also demonstrates the potential as well as the limitations of the LA-ICPMS U-Pb zircon analysis. Limitations include the lack of ideal reference materials to correct for instrumental and mass bias, the uncertainty in the ablation behavior of different zircons and the U/Pb heterogeneity in zircon grains.

5 Conclusions

LA-ICPMS has become one of the most promising techniques for multi-element analysis of geochemical, cosmochemical, biological and environmental samples. It is very well suited for microanalysis, and it is also suited for bulk analysis using homogeneous samples, such as fused glasses. High sensitivity is important, especially for small spots and low trace element contents. Single-collector sector-field and quadrupole instruments are useful for quantitative elemental analysis and moderate precision isotopic work, whereas multi-collector sector-field instruments are needed for the high-precision isotope ratio measurements.

The detector components are the weakest links in the system, and hopefully the future may see some

innovative devices[19]. The limitations of present day detectors include settling time, linearity, stability, and dynamic range. State-of-the-art laser systems are Nd: YAG and ArF excimer lasers with 213 nm, 193 nm wavelengths and ns pulse widths. However, one of the main limitations of LA-ICPMS is the occurrence of non-stoichiometric effects in the transient signals, defined as elemental fractionation. Moreover, matrix effects, non-linear calibrations, and the lack of suitable certified reference materials are other possible limitations. The developments of lasers have therefore been driven in the direction of shorter pulses[43]. In the case of fs laser ablation, the shortening of the laser pulses leads to a shrinking of the heat-affected zone. The affected material is fully removed with no or minimal damage to the surrounding area. Up to now fs lasers have been successfully used for some geochemical, mainly isotopic, applications. However, fs laser ablation has not yet been proven undoubtedly to eliminate elemental or isotopic fractionation[19].

6 References

[1] Sylvester P (ed). Laser Ablation-ICP-MS in the Earth Sciences: Current practices and outstanding issues. Min Ass Canada, Short Course Series, 2001, 29: 243.

[2] Lipschutz M E, Wolf S F, Culp F B, Kent A J R. Geochemical and Cosmochemial Materials [J]. *Anal Chem*, 2007, 79: 4249 – 4274.

[3] Jochum K P, Nohl U, Herwig K, Lammel E, Stoll B, Hofmann A W. GeoReM: A new geochemical database for reference materials and isotopic standards [J]. *Geostand Geoanalyt Res*, 2005,29: 333 – 338.

[4] Szynkowska M I, Czerski K, Paryjczak T, Rybicki E, Wlochowicz A. Testing textiles using the LA-ICPMS-TOF method[J]. *Fibres and Textiles in Eastern Europe*, 2006, 14: 87 – 90.

[5] Guillong M, Günther D. Effect of particle size distribution on ICP-induced elemental fractionation in laser ablation-inductively coupled plasma-mass spectrometry[J]. *J Anal At Spectrom*, 2002, 17: 831 – 837.

[6] Horn I, von Blanckenburg F, Schoenberg R, Steinhoefel G, Markl G. In situ iron isotope ratio determination using UV-femtosecond laser ablation with application to hydrothermal ore formation processes [J]. *Geochim Cosmochim Acta*, 2006, 70: 3677 – 3688.

[7] Poitrasson F, Mao X L, Mao S S, Freydier R, Russo R E. Comparison of ultraviolet femtosecond and nanosecond laser ablation inductively coupled plasma mass spectrometry analysis in glass, monazite, and zircon[J]. *Anal Chem*, 2003, 75: 6184 – 6190.

[8] Mozna V, Pisonero J, Hola M, Kanicky V, Günther D. Quantitative analysis of Fe-based samples using ultraviolet nanosecond and femtosecond laser ablation-ICP-MS[J]. *J Anal At Spectrom*, 2006, 21: 1194 – 1201.

[9] Jochum K P, Stoll B, Herwig K, Willbold M. Validation of LA-ICPMS trace element analysis of geological glasses using a new solid-state 193 nm Nd: YAG laser and matrix-matched calibration[J]. *J Anal At Spectrom*, 2007, 22: 112 – 121.

[10] Regnery J. Neues Verfahren in der Laserablation-ICP-Massenspektrometrie zur Bestimmung von Elementkonzentrationen in geologischen Proben mit Hilfe hochaufgelöster Massenspektren [D]. Germany: University of Mainz, 2008.

[11] National Institute of Standards and Technology. Certificate of Analysis Standard Reference Material 982, Gaithersburg (May W E, Karam L R, Watters Jr R L), 2004.

[12] Jochum K P and 5 2 coauthors. MPI - DING reference glasses for in situ microanalysis: New reference values for element concentrations and isotope ratios [J]. *Geochem Geophys Geosyst*, 2006, 7(2): doi: 101029/2005GC001060.

[13] Jochum K P, Stoll B, Herwig K, Amini M, Abouchami W, Hofmann AW. Lead isotope ratio measurements in geological glasses by laser ablation-sector field-ICP mass spectrometry (LA-SF-ICPMS) [J]. *Int J Mass Spectrom*, 2005, 242: 281 – 289.

[14] Jochum K P, Stoll B, Herwig K, Willbold M. Improvement of in situ Pb isotope analysis by LA-ICPMS using a 193 nm Nd:YAG laser[J]. *J Anal At Spectrom*, 2006, 21: 666 – 675.

[15] Paul B, Woodhead J D, Hergt J. Improved in situ isotope analysis of low-Pb materials using LA-MC-ICP-MS with parallel ion counter and Faraday detection[J]. *J Anal At Spectrom*, 2005, 20: 1350 – 1357.

[16] Jochum K P, Sobolev A V, Kuzmin D, Hofmann A W. A sensitive LA-ICPMS technique for Sr and Pb isotope analysis using a new solid-state 193 nm laser and application to Mauna Loa melt inclusions[J]. *Eos Trans AGU*, 2006, 87(52), Fall Meet Suppl.

[17] Hattendorf B, Latkoczy C, Günther D. Laser ablation-ICPMS[J]. *Anal Chem*, 2003,75(15): 341A – 347A.

[18] Fryer B F, Jackson S E, Longerich H P. The design, operation and role of the laser-ablation microprobe coupled with an inductively coupled plasma-mass spectrometer (LAM-ICP-MS) in the Earth sciences[J]. *Can Mineral*, 1995, 33: 303 – 312.

[19] Sylvester P (ed). Laser ablation-ICP-MS in the earth sciences: Current practices and outstanding Issues. Min Ass Canada, Short Course Series, 2008, 40: 348.

[20] Pearce N J G, Perkins W T, Westgate J A, Gorton M P, Jackson S E, Neal C R, Chenery S P. A compilation of new and published major and trace element data for NIST SRM 610 and NIST SRM 612 glass reference

materials[J]. *Geostand Newslett*, 1997, 21: 115 – 144.

[21] Kane J S. Fitness - for - purpose of reference material reference values in relation to traceability of measurement, as illustrated by USGS BCR-1, NIST SRM 610 and IAEA NBS28 [J]. *Geostand Newslett*, 2002, 26: 7 – 29.

[22] Jochum K P, Willbold M, Raczek I, Stoll B, Herwig K. Chemical characterisation of the USGS reference glasses GSA-1G, GSC-1G, GSD-1G, GSE-1G, BCR-2G, BHVO-2G and BIR-1G using EPMA, ID-TIMS, ID-ICPMS and LA-ICPMS[J]. *Geostand Geoanal Res*, 2005, 29: 285 – 302.

[23] Guillong M, Hametner K, Reusser E, Wilson S A, Günther D. Preliminary characterisation of new glass reference materials (GSA-1G, GSC-1G, GSD-1G and GSE-1G) by laser ablation-inductively coupled plasma-mass spectrometry using 193 nm, 213 nm and 266 nm wavelengths [J]. *Geostand Geoanal Res*, 2005, 29: 315 – 331.

[24] Cotta A J B, Enzweiler J. Certificate of analysis of the reference material BRP-1 (Basalt Ribeirao Preto)[J]. *Geostand Geoanal Res*, 2008, 32: 231-235.

[25] Latkoczy C, Becker S, Dücking M, Günther D, Hoogewerff J A, Almirall J R, Buscaglia J, Dobney A, Koons R D, Montero S, van der Peijl G J Q, Stoecklein W R S, Trejos T, Watling J R, Zdanowicz V S. Development and evaluation of a standard method fort he quantitative determination of elements in float glass samples by LA-ICPMS[J]. *J Forensic Sci*, 2005, 50: 1327 – 1341.

[26] Fedorowich J S, Richards J P, Kain J C, Kerrich R, Fan J. A rapid method for REE and trace element analysis using laser sampling ICP-MS on direct fusion whole-rock glasses[J]. *Chem Geol*, 1993, 106: 229 – 249.

[27] Stoll B, Jochum K P, Herwig K, Amini M, Flanz M, Kreuzburg B, Kuzmin D, Willbold M, Enzweiler J. An automated iridium-strip heater for LA-ICPMS bulk analysis of geological samples [J]. *Geostand Geoanal Res*, 2008, 32: 5 – 26.

[28] Cotta A J B, Enzweiler J, Wilson S A, Pérez C A, Nardy A J R, Larizzatti J H. Homogeneity of the geochemical reference material BRP-1 (Paran Basin basalt) and assessment of minimum mass[J]. *Geostand Geoanal Res*, 2007, 31: 379 – 393.

[29] Stolper E M, DePaolo D J, Thomas D M. Introduction to special section: Hawaii Scientific Drilling Project [J]. *J Geophys Res*, 1996, 101: 11593 – 11598.

[30] Hofmann A W, Jochum K P. Source characteristics derived from very incompatible trace elements in Mauna Loa and Mauna Kea basalts, Hawaii Scientific Drilling Project[J]. *J Geophys Res*, 1996, 101: 11831 – 11839.

[31] Amini M . Geochemistry of fresh submarine glasses from the Hawaii Scientific Drilling Project-2 [D]. Germany: University of Mainz, 2003.

[32] Eisele J, Abouchami W, Galer S J G, Hofmann A W. The 320 kyr Pb isotope evolution of Mauna Kea lavas recorded in the HSDP-2 drill core[J]. *Geochem Geophys Geosyst*, 2003, 4(5), doi:101029/2002GC000339.

[33] Sobolev A V, Hofmann A W, Nikogosian I K. Recycled oceanic crust observed in ghost plagioclase within the source of Mauna Loa lavas [J]. *Nature*, 2000, 404: 986 – 990.

[34] Ionov D, Blichert - Toft J, Weis D. Hf isotope compositions and HREE variations in off-craton garnet and spinel peridotite xenoliths from central Asia[J]. *Geochim Cosmochim Acta*, 2005, 69: 2399 – 2418.

[35] Ionov D, Ashchepkov I, Jagoutz E, Wiecher U. The provenance of fertile off-craton lithospheric mantle: Sr-Nd isotope and chemical composition of garnet and spinel peridotite xenoliths from Vitim, Siberia [J]. *Chem Geol*, 2005, 217: 41 – 75.

[36] Jochum K P, Stoll B, Amini M, Palme H. Limited trace element fractionation in SNC meteorites [J]. *Meteoritics and Planet Sci*, 2001, 36 (Suppl): A90 – A91.

[37] Amelin Y, Krot A N, Hucheon I D, Ulyanov A A. Lead isotopic ages of chomdrules and calcium-aluminum-rich inclusions [J]. *Science*, 2002, 297: 1678 – 1683.

[38] Jochum K P, Friedrich J M, Ebel D S, Galer S J G. Heterogeneous Th-U-Pb isotope and elemental systematics in calcium-aluminum-rich inclusions determined by LA-ICPMS[J]. *Meteoritics and Planet Sci*, 2005, 40 (Suppl): A76

[39] Müller W E G, Jochum K P, Stoll B, Wang X. Formation of giant spicule from quartz glass by the deep sea sponge Monorhaphis[J]. *Chemistry of Materials*, 2008, 20: 4703 – 4711.

[40] Mertz - Kraus R, Brachert T C, Galer S J, Stoll B, Jochum K P, Reuter M. Late Miocene freshwater runoff seasonality inferred by LA-ICPMS and TIMS analyses on Eastern Mediterranean corals[J]. *Eos Trans AGU*, 2007, 88, Fall Meet Suppl, Abstract PP31D – 0657.

[41] Brachert T C, Reuter M, Felis T, Kroeger K F, Lohmann G, Micheels A, Fassoulas C. *Porites* corals from Crete (Greece) open a window into Late Miocene (10 Ma) seasonal and interannual climate variability [J]. *Earth Planet Sci Lett*, 2006, 245: 81-94.

[42] Chang Z, Vervoort J D, McClelland W C, Knaack C. U-Pb dating of zircon by LA-ICPMS[J]. *Geochem Geophys Geosyst*, 2006, 7, doi:10.1029/2005GC001100.

[43] Fernández B, Claverie F, Pécheyran C, Donard O F X. Direct analysis of solid samples by fs-LA-ICPMS [J]. *Trends Anal Chem*, 2007, 26: 951 – 966.